ZAMM · Z. Angew. Math. Mech. **87**, No. 1, 24 – 36 (2007) / **DOI** 10.1002/zamm.200510293

Wax diffusivity under given thermal gradient: a mathematical model

Sebastiano Correra[1], **Antonio Fasano** [2], **Lorenzo Fusi**[2,*], **Mario Primicerio**[2], **and Fabio Rosso** [2]

[1] EniTecnologie, Via F. Maritano, 20097, San Donato Milanese, Milano, Italy
[2] I2T3, Dipartimento di Matematica "U.Dini", Università di Firenze, Viale Morgagni 67/A, 50134 Firenze, Italy

Received 9 November 2005, revised 14 June 2006, accepted 6 September 2006
Published online 10 November 2006

Key words Heat and mass transfer, diffusion, free boundary problems
MSC (2000) 80A20, 76R50, 35R35

In this paper we describe how to obtain wax diffusivity and solubility in a saturated crude oil using the measurements of solid wax deposit in the experimental apparatus known as cold finger. Assuming that migration of dissolved wax is primarily driven by thermal gradients, a mathematical model is derived relating the deposit growth rate to the above mentioned quantities. We investigate the case in which the oil is not agitated. Comparisons with available experimental data are performed and possible sources of errors are discussed.

1 Introduction

Waxy crude oils (WCO's) are mineral oils containing a sufficiently large amount of wax (a complex mixture of heavy hydrocarbons), a property that is going to affect pipelining operations under particular thermal conditions. This peculiar feature of WCO's is due to the fact that when temperature drops below the so-called *cloud point* $T_{\rm cloud}$ (or WAT = wax appearing temperature) wax crystals appear, which at an even lower temperature (*pour point*) develop a strong tendency to aggregate forming a gel structure. Obviously, this feature influences rheology in a quite significant way (see the review paper [4]).

Besides rheological complications another relevant process taking place when radial thermal gradients are present in the pipeline (a typical situation for submarine ducts) is the growth of a solid wax deposit at the wall due to molecular diffusion. This has to be predicted with some accuracy for planning periodic removal of the deposit. This delicate question has been considered in the recent paper [3] for the case of turbulent flux. We refer to it also for some bibliographical references. The main physical parameters of a WCO that have to be known to predict the deposit growth rate are the *diffusivity* of dissolved wax and the *solubility* (i.e. that saturation concentration as a function of temperature). An experimental apparatus used to obtain diffusivity (but also solubility) through measures of the wax deposit is the so-called *cold finger*. This device is designed to measure the mass deposit from oil samples, occurred over given time intervals under controlled temperature gradients.

The aim of this paper is to write down predictive formulas for the wax deposit in a cold finger device and to show how to use them to deduce the values of the desired parameters from deposit measurements. In particular we will point out how to obtain the maximum amount of information from the available experimental data and we will discuss with some care the range of applicability of the cold finger devices. The case considered here is the the one in which the sample is not stirred (static device).

Our main scope is to provide insight of the basic mechanism determining wax deposition on cold walls. Since our claim is that the relevant physical factor in the phenomenon is thermal gradient (see [1] for an extensive discussion), we will write a mathematical model in which other effects are neglected not because they are absent but because their presence is not crucial for the correct interpretation of the experiments. In particular, kinetics of wax crystallization and dissolution are considered to be very fast in comparison with mass transport (this assumption is implicitly done in all the previous literature on this topic).

Moreover, we will consider wax as formed by a single component and we assume that oil and wax (both in the segregated and dissolved phase) have the same density ρ, so that no gravity settling nor volume change occur because of crystallization or deposition.

* Corresponding author, e-mail: fusi@math.unifi.it, Phone: +00 39 55 4237133, Fax: 00 39 55 4237133

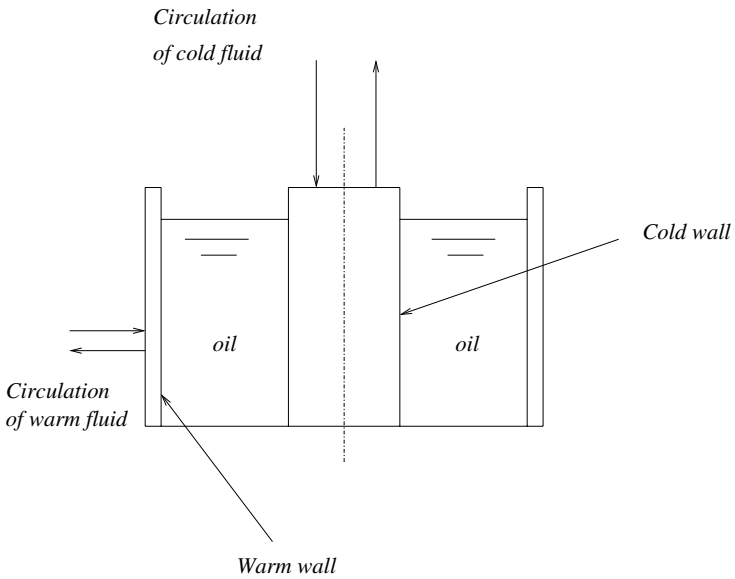

Fig. 1 Sketch of the cold finger.

Making use of the experimental results reported in [2] we will show how to evaluate wax diffusivity from various oils, reaching the conclusion that in the static device only the contribution of the light fraction of wax is visible.

2 Description of the apparatus

The apparatus consists in a cylindrical container (typical radius $\approx$ 12 cm) whose lateral wall can be kept at a selected temperature, and of another thermally controllable cylinder (the cold finger, radius ≈ 5 cm), inserted along the same axis and destined to collect the deposit (see Fig. 1). Other configurations have also been used (see [10]).

The oil sample is initially placed in a thermostatic bath and then warmed to $30 \div 40$ K over its WAT, in order to homogenize the material and to erase its "thermal" and "mechanical" history. After a sufficiently long time (usually a few hours), the sample is cooled to the temperature T_e that will be kept constant at the external wall during the experiment. At this point the cold finger (a metallic cylinder which is kept at constant temperature $T_i < T_e$) is immersed in the sample so that an axially symmetric thermal field through the sample is produced.

Due to the large difference between thermal and mass diffusion, the thermal transient is negligible (with respect to the concentration transient) and a steady-state profile is assumed for the temperature.

We denote by $C_s(T)$ the wax saturation concentration at the temperature T, i.e. the maximum mass of wax that can be dissolved in a unit volume of the given oil. $C_s(T)$ is an increasing function. When total wax concentration $c_{\rm tot}$ exceeds C_s a segregated phase will appear (in form of suspended crystals) and the solution is *saturated*. The corresponding concentration of the segregated phase will be denoted by $G = c_{\rm tot} - C_s$. Let $c^*_{\rm tot}$ be the initial concentration of wax in the sample. If the temperature of the cold finger is above $T_{\rm cloud}$ no segregated phase will appear (the solution is unsaturated throughout the sample at these temperatures) and the concentration of the dissolved wax will remain constant and equal to $c^*_{\rm tot}$.

On the contrary if the temperature of the outer surface is below $T_{\rm cloud}$, all the solution will be initially saturated and the concentration of the dissolved wax will be determined by the temperature profile within the sample. Excess wax will be present as crystallized segregated phase.

In the intermediate case, $T_i < T_{\rm cloud} < T_e$, there will be a surface separating the unsaturated region (close to the outer cylinder) and the saturated region (in the vicinity of the cold finger).

Excluding the first case $T_i > T_{\rm cloud}$, since C_s is an increasing function of temperature and since we have created a thermal gradient in the sample, a gradient in the concentration of the dissolved wax will exist. Hence the latter diffuses towards the cold wall. Once the transported material comes in touch with the cold wall it adheres to the surface, thus forming a solid layer which does not appreciably modify geometry of the system, since its thickness is usually much smaller than the cold finger radius. This mechanism of mass transport through a WCO is known as *molecular diffusion*. Other deposition mechanisms may contribute to the formation of deposits, like shear dispersion, Brownian diffusion and gravity settling. However there is a general agreement in considering molecular diffusion to be dominant in the present conditions (see [7]). This is the reason why, in our analysis, we focus on this mechanism only.

The aim of the experiment is to measure, for a given oil, the amount of deposit at different times and for different temperature gradients.

In our analysis we shall consider the situation in which the oil is immobile[1]. The system goes through several stages. If initially it is completely saturated, the mass current in the solution which leaves the warm wall to reach the cold finger is fed by the segregated phase (as long as the concentration of the latter stays positive) in order to keep thermodynamical equilibrium between dissolved and segregated phase. This stage is followed by progressive desaturation with depletion of the segregated phase and eventually the system becomes totally desaturated. The wax concentration tends asymptotically to the saturation concentration corresponding to the cold finger temperature.

We will discuss possible sources of errors and we will also suggest a standard procedure to extrapolate the long time behavior of the device (not always experimentally available) from measures taken in the stages preceding total desaturation. Since in many cases attaining the asymptotic behavior requires a too long time, the above information is of practical interest.

3 Temperature, concentrations, solubility, and diffusivity

3.1 Temperature and concentrations

Temperature will be considered independent of time, since, as mentioned in the introduction, it reaches its steady state before any significant mass transfer occurs. The thermal profile will not change since the change of enthalpy occurring during segregation/dissolution with respect to the heat flux determined by the two thermostats is negligible (see [3]). We denote by r the radial coordinate and by R_i and R_e the radius of the cold finger and of the outer wall. We have

$$T(r) = T_i + \frac{(T_e - T_i)}{\ln\left(\dfrac{R_e}{R_i}\right)} \ln\left(\frac{r}{R_i}\right), \tag{1}$$

where we recall $T_e > T_i$ represent the constant temperatures at the outer (warm) and at the inner (cold) walls.

We suppose that all concentrations and temperature do not depend on the axial coordinate and we introduce:

- $c_{\rm tot}(r,t)$ total wax concentration,
- $c_{\rm tot}(r,0) = c^*_{\rm tot}$ initial total wax concentration,
- $c(r,t)$ dissolved wax concentration,
- $G(r,t)$ segregated wax concentration,
- $C_s(T(r))$ saturation concentration (solubility).

By definition

$$G(r,t) = \left[c_{\rm tot}(r,t) - C_s(T(r))\right]_+, \tag{2}$$

where $[..]_+$ denotes the positive part and is equal to zero when the quantity in brackets is negative,

$$c_{\rm tot}(r,t) = G(r,t) + c(r,t), \tag{3}$$

$$c(r,t) = \min\{c_{\rm tot}(r,t), C_s(T(r))\}. \tag{4}$$

The dependence of solubility C_s on temperature could be theoretically inferred from the thermodynamics of mixtures.

By assuming an ideal behaviour of the bicomponent mixture (see [9]) we have

$$C_s(T) = C_s(T_{\rm cloud}) \exp\left\{-\frac{\lambda}{R}\left(\frac{1}{T} - \frac{1}{T_{\rm cloud}}\right)\right\}, \tag{5}$$

where λ is the wax latent heat and R is the gas constant. Applying Taylor's expansion around the cloud point we get

$$C_s(T) = C_s(T_{\rm cloud})\left\{1 + \frac{\lambda}{RT^2_{\rm cloud}}(T - T_{\rm cloud}) + \frac{\lambda}{RT^3_{\rm cloud}}\left[\frac{\lambda}{2RT_{\rm cloud}} - 1\right](T - T_{\rm cloud})^2 + ...\right\}. \tag{6}$$

The ratio between the quadratic and the linear term in expression (6) is

$$\Psi = \frac{1}{T_{\rm cloud}}\left[\frac{\lambda}{2RT_{\rm cloud}} - 1\right](T - T_{\rm cloud}). \tag{7}$$

[1] We neglect convective motions possibly induced within the inhomogeneous thermal field, although such disturbances may have some influence on the computed value of wax diffusivity.

Using typical values $\lambda = 5.4$ cal/g, $R = 1.9$ cal/Mole· K, $T_{\rm cloud} = 300$ K, a molecular weight $MW = 410$ g/mol and a maximum $|T - T_{\rm cloud}| = 30$ K (the range of temperatures we will consider), we have

$$|\Psi| = 9.5 \cdot 10^{-2}. \tag{8}$$

Thus a linear approximation is justified and we will write

$$C_s(T) = C_s(T_i) + b_w(T - T_i). \tag{9}$$

We use this argument as a theoretical basis for (9), but we will determine the constant b_w from experiments.

We assume that the initial concentration $c^*_{\rm tot} > 0$ is constant and we suppose $C_s(T_i) < c^*_{\rm tot}$, that ensures that near the cold wall the solution is saturated. In this region a radial gradient of dissolved wax is formed and the latter is transported to the cold wall by molecular diffusion and sticks to the cold finger (see (13)). The system will evolve through three stages

- STAGE 1 – Saturation through the whole sample,
- STAGE 2 – Partial saturation,
- STAGE 3 – Complete desaturation.

Of course Stage 1 only exists if $c^*_{\rm tot} > C_s(T_e)$. Otherwise the evolution starts from Stage 2. During Stages 1 and 2 the deposit growth rate is constant (mass grows linearly with time), while in Stage 3 it tends asymptotically to 0.

3.2 Determining solubility and diffusivity from deposition measures

It is known that the deposit is formed by wax and entrapped oil. In the static device wax crystals tend to form a rather thin structure so that the oil fraction in the deposit is usually quite large.

We denote by ϕ the mass fraction of wax in the deposit and we define $m_\infty(T_i)$ to be the asymptotic value (i.e. measured at time when the deposit growth rate is no longer appreciable) of the mass (per unit surface) deposited on the cold wall kept at temperature T_i . We have

$$m_\infty(T_i) = m_{\infty w}(T_i) + m_{\infty o}(T_i), \tag{10}$$

where

$$m_{\infty w}(T_i) =: \phi m_\infty(T_i),$$

$$m_{\infty o}(T_i) =: (1 - \phi) m_\infty(T_i)$$

represent the asymptotic mass of wax and oil in the deposit. The wax fraction ϕ can be rather small (becoming an important source of errors) and will be considered constant in the range of temperatures of the experiment. We also have

$$m_{\infty w}(T_i) = (c^*_{\rm tot} - C_s(T_i)) \cdot \frac{(R_e^2 - R_i^2)}{2R_i}, \tag{11}$$

hence, when solubility is approximated by (9) and T_{i1}, T_{i2} denote two different temperatures of the cold finger, we have

$$b_w = \frac{(m_{\infty w}(T_{i1}) - m_{\infty w}(T_{i2}))2R_i}{(R_e^2 - R_i^2)(T_{i2} - T_{i1})} = \phi \underbrace{\left[\frac{m_\infty(T_{i1}) - m_\infty(T_{i2})}{(T_{i2} - T_{i1})}\right]}_{=b} \cdot \frac{2R_i}{(R_e^2 - R_i^2)} = \frac{\phi b 2R_i}{(R_e^2 - R_i^2)}. \tag{12}$$

Thus the solubility derivative b_w can be determined once we know ϕ and two measures of the total deposited mass for two different temperatures of the cold finger. We notice that the measure of $c^*_{\rm tot}$ does not enter (12).

Let us denote by $m(t)$ the total deposited mass per unit surface at time t. Once more $m_w(t) = \phi m(t)$ and $m_o = (1 - \phi)m(t)$ are the wax and oil deposited mass respectively. According to the assumption that molecular diffusion is the only driving mechanism for wax migration to the wall, the deposition rate $\dot m_w$ (rate at which wax deposits per unit surface) is given by

$$\dot m_w = \phi \dot m = D_w \left.\frac{\partial c}{\partial r}(r,t)\right|_{r=R_i}, \tag{13}$$

where $\dot{m} = dm/dt$, and D_w is wax diffusivity. When the solution is saturated in the vicinity of the cold finger c has to be replaced by C_s and (13) becomes

$$\dot{m}_w = D_w b_w \left.\frac{dT}{dr}\right|_{r=R_i} = D_w b_w \frac{(T_e - T_i)}{\ln\left(\dfrac{R_e}{R_i}\right)} \frac{1}{R_i}. \tag{14}$$

As long as the region near the cold finger remains saturated mass grows linearly with time. From (14) it is clear the importance of knowing the product $D_w b_w$ for predicting the amount of deposit or vice-versa, how to estimate D_w from the deposition rate.

If we know the amount of deposit per unit surface $m^* =: \phi^{-1} m_w^*$ for a fixed time t^* during the linear growth regime, then we can determine the diffusivity coefficient D_w using

$$D_w = \frac{m_w^*}{t^*} \frac{1}{b_w T_r(R_i)} = \frac{m^*}{t^*} \frac{R_e^2 - R_i^2}{2 R_i b T_r(R_i)}, \tag{15}$$

where b (or b_w) is obtained by means of the procedure previously explained. It is important to remark that only b and m^* (i.e. the total deposited mass) determine D_w, making it independent of the value of ϕ as well as of $c_{\rm tot}^*$. Moreover, since $T_{\rm cloud}$ is defined to be such that

$$C_s(T_{\rm cloud}) = c_{\rm tot}^*, \tag{16}$$

then from (11)

$$T_{\rm cloud} = T_i + \frac{m_{\infty w}(T_i)}{b_w} \cdot \frac{2R_i}{(R_e^2 - R_i^2)} = T_i + \frac{m_\infty(T_i)}{b}. \tag{17}$$

In [2] experimental data are given referring to six samples of different oils A, B, C, D, E, F and measures of deposited mass are displayed as a function of time and for assigned temperatures.

We use these data to get the asymptotic values $m_\infty(T_i)$, making use, when needed, of the extrapolation technique described in Appendix 2. Then we compute b_w and $T_{\rm cloud}$ for the six oils using (12) and (17), respectively. The corresponding results are displayed in Table 1 together with the experimental values of $c_{\rm tot}^*$, $T_{\rm cloud}$ given in [2]. Comparison of values in columns 2 and 3 shows that our approximation is reasonable.

We note that formula (17) uses the ratio $m_\infty(T_i)/b$ and thus the derived value of $T_{\rm cloud}$ refers in practice just to the fraction of wax that has actually reached the cold finger. This explains why (17) gives values of $T_{\rm cloud}$ slightly lower than the ones obtained by direct measures (see Table 1).

Table 1 Cloud point and solubility gradient for oil samples A–F.

Oil;	$c_{\rm tot}^*$ from [2], [kg/m^3]	$T_{\rm cloud}$ from [2], [K];	$T_{\rm cloud}$ using (17) [K];	b_w, [kg/m^3/K]
A	20.25	303	299	0.006
B	34.02	306	305	0.011
C	58.30	315	312	0.021
D	62.37	312	310	0.0035
E	90.72	308	307	0.0058
F	97.20	323	322	0.0014

In Fig. 3 of [8] solubility as a function of temperature is plotted for a crude oil with physical properties similar to oil A of [2], confirming that, in the range of temperature of our experiments, a linear approximation for C_s is reasonable. Further if we compute the average slope we obtain a value of b_w in the same range as the ones reported in Table 1.

Actually a better fitting may be obtained with a quadratic polynomial (and this could be done in analytical treatment and numerical simulation). However we have already outlined the spirit of this paper in the introduction: to describe the simplest model incorporating the minimum number of parameters and mechanisms apt to explain the phenomenon under consideration, also taking into account that an error of 10 % on data is an optimistic expectation of their accuracy.

The most natural way of determining D_w is to use measurements of deposited mass during the early stage of the phenomenon (Stages 1 and 2) when the deposit rate is constant. Using the values of b_w obtained in Table 1 we compute the values of D_w resulting from the different experiments, obtaining Table 2.

Table 2 Diffusivity values for different cold finger temperatures.

Oil	$(T_e - T_i)$ [K]	T_i [K]	T_e [K]	Starting stage	Wax diffusivity $D_w[\mathrm{m}^2/\mathrm{s}]$
A	10	278	288	1	3.20×10^{-7}
A	15	278	293	1	3.20×10^{-7}
A	10	298	308	2	3.51×10^{-8}
B	25	288	313	2	8.67×10^{-8}
B	20	293	313	2	3.21×10^{-8}
C	30	288	318	2	1.24×10^{-7}
C	25	293	318	2	6.80×10^{-8}
D	25	290	315	2	1.35×10^{-7}
D	20	295	315	2	8.48×10^{-8}
E	24	289	313	2	1.30×10^{-7}
E	19	294	313	2	5.70×10^{-8}
F	15	313	328	2	8.12×10^{-8}
F	10	318	328	2	8.10×10^{-8}

The computed wax diffusivity for oil A in case $T_i = 298$ K and $T_e - T_i = 10$ K is not significant, since the difference $T_{\mathrm{cloud}} - T_i$ is very small (1 K), meaning that the duration of the stage of linear growth is too short to be identified. Of course we refer to the value T_{cloud} consistent with the model. This implies that the first mass measure (the one taken after 4 hours) is taken when the system has reached or is approaching the asymptotic stage (Stage 3) and thus not usable for evaluating D_w (the computed value is in fact smaller than the one from experiments 1 and 2).

We note that the diffusivity values in Table 2 are systematically greater than the values usually assumed in field calculations. In particular it emerges that D_w is a decreasing function of T_i. In Table 3 it is shown the decrease of D_w due to an increase of the cold wall temperature.

Table 3 Decrease of D_w with T_i.

Oil	Decrease of D_w (per K)	Oil	Decrease of D_w (per K)
A	–	D	8%
B	9%	E	10%
C	7%	F	2%

The dependence of D_w on T_i is due to the fact that at lower temperatures the fraction of lighter wax components contributing to the phenomenon is larger. Since D_w expresses an overall property, this explains its (otherwise unexpected) behaviour. This fact has been already explained in [2]. We remark anyway that in our analysis the variation of D_w with T_i is much more restrained than in [2]. In Appendix 3 we show how to get a priori bounds for D_w.

4 The mathematical model

Here we formulate the mathematical model assuming that the system evolves from Stage 1, i.e. $T_e < T_{\mathrm{cloud}}$. The thickness of the deposit layer is neglected and at any time the deposition front is given by $r = R_i$.

4.1 Stage 1

We suppose that at time $t = 0$ the solution is everywhere saturated by wax, that is $G(r, 0) = G_o(r) > 0$ in $[R_i, R_e]$. The balance equations are

$$\frac{\partial G}{\partial t} - D_G \left(\frac{\partial^2 G}{\partial r^2} + \frac{1}{r} \frac{\partial G}{\partial r} \right) = Q, \tag{18}$$

$$-D_w \left(\frac{\partial^2 C_s}{\partial r^2} + \frac{1}{r} \frac{\partial C_s}{\partial r} \right) = -Q, \tag{19}$$

where Q is the transition rate from dissolved to segregated phase per unit volume and D_G is diffusivity of the segregated phase. From (1), (9) and from (19) we obtain

$$\left(\frac{\partial^2 C_s}{\partial r^2} + \frac{1}{r}\frac{\partial C_s}{\partial r}\right) = C_s^{'}\left(\frac{d^2 T}{dr^2} + \frac{1}{r}\frac{dT}{dr}\right) = 0, \tag{20}$$

where $C_s^{'} = dC_s/dT = b_w$. From (20) we get $Q = 0$. Thus during Stage 1 G satisfies the parabolic equation

$$\frac{\partial G}{\partial t} - D_G\left(\frac{\partial^2 G}{\partial r^2} + \frac{1}{r}\frac{\partial G}{\partial r}\right) = 0 \tag{21}$$

with initial data

$$0 < G(r,0) = G_o(r) = c^*_{\mathrm{tot}} - C_s(T(r)) < \rho, \tag{22}$$

where we recall that ρ is density. The boundary condition on $r = R_e$ expresses mass balance

$$D_G\frac{\partial G}{\partial r}(R_e,t) = -D_w b_w \frac{dT}{dr}(R_e) = -\frac{D_w b_w}{R_e}\frac{(T_e - T_i)}{\ln(R_e/R_i)} < 0. \tag{23}$$

For $r = R_i$ we simply have

$$\frac{\partial G}{\partial r}(R_i,t) = 0, \tag{24}$$

meaning that all the solute incoming mass enters the deposit at the cold finger with no "recirculation". Stage 1 ends at time t_1 when $G(R_e,t_1) = 0$. During this stage the wax deposition rate is given by (14) (we recall that the total deposition rate is obtained dividing wax deposition rate by ϕ). With reference to Table 1 and 2 we note that Stage 1 is present only in the first two experiments performed with oil A.

4.2 Stage 2

At time $t_1 > 0$ a desaturation front $r = s(t)$, starting from the warm wall $s(t_1) = R_e$ and moving towards the cold wall, is generated. The function $s(t)$ is unknown. When $s(t)$ reaches $r = R_i$ Stage 2 ends and the solution is everywhere unsaturated. During Stage 2 we must solve the equations for the saturated and unsaturated phase, that is

$$\frac{\partial G}{\partial t} - D_G\left(\frac{\partial^2 G}{\partial r^2} + \frac{1}{r}\frac{\partial G}{\partial r}\right) = 0, \qquad R_i < r < s(t), \quad t_1 < t < t_2, \tag{25}$$

$$\frac{\partial c}{\partial t} - D_w\left(\frac{\partial^2 c}{\partial r^2} + \frac{1}{r}\frac{\partial c}{\partial r}\right) = 0, \qquad s(t) < r < R_e, \quad t_1 < t < t_2. \tag{26}$$

For $t = t_1$ the function G is obtained from Stage 1, i.e. $G(r,t_1)$. The boundary conditions are given imposing the absence of flux at the walls

$$\frac{\partial c}{\partial r}(R_e,t) = 0, \qquad \frac{\partial G}{\partial r}(R_i,t) = 0. \tag{27}$$

On the moving boundary $r = s(t)$ we have

$$G(s,t) = 0, \tag{28}$$

$$D_w\frac{\partial c}{\partial r}(s,t) - D_w b_w \frac{dT}{dr}(s) = D_G\frac{\partial G}{\partial r}(s,t), \tag{29}$$

where (28) and (29) express the absence of segregated phase and the continuity of total flux on the desaturation front, respectively. The end of Stage 2 is marked by the time $t_2 > t_1$ such that $s(t_2) = R_i$. Also during this stage the deposition rate is given by (14).

4.3 Stage 3

Stage 3 is characterized by complete desaturation. The initial condition for the solute concentration comes from Stage 2, i.e. $c(r, t_2)$. The equation to be solved is the one of the unsaturated phase

$$\frac{\partial c}{\partial t} - D_w \left(\frac{\partial^2 c}{\partial r^2} + \frac{1}{r} \frac{\partial c}{\partial r} \right) = 0, \qquad R_i < r < R_e, \quad t > t_2, \tag{30}$$

with boundary conditions

$$\frac{\partial c}{\partial r}(R_e, t) = 0, \qquad c(R_i) = C_s(T_i). \tag{31}$$

During Stage 3 wax (and also total) deposition rate $\dot{m}_w$ tends asymptotically to 0 and it is expressed by

$$\dot{m}_w = D_w \frac{\partial c}{\partial r}(R_i, t). \tag{32}$$

Differently from previous stages it is now impossible to write down an explicit expression for wax deposition rate, but we can solve the problem numerically.

Remark 1. The knowledge of wax deposition rate during all stages is necessary to study the growth of the deposit layer. The amount of deposited wax per unit surface and per unit time is

$$D_w \frac{\partial c}{\partial r}(R_i, t), \tag{33}$$

where c is given by $C_s(T)$ during the first two stages and by the solution of (30)-(31) during the third. Assuming that the solution is initially everywhere saturated (the system evolves from Stage 1) the deposited mass per unit surface m is given, for any $t > t_2$ (i.e. during Stage 3), by

$$m_w = D_w b_w \frac{(T_e - T_i)}{\ln\left(\dfrac{R_e}{R_i}\right)} \frac{1}{R_i} t_2 + \int_{t_2}^{t} D_w \frac{\partial c}{\partial r}(R_i, \tau) d\tau. \tag{34}$$

In case the system evolves from Stage 2 time t_2 in (34) indicates the duration of Stage 2 only. Of course the total deposit is given by $m = m_w/\phi$.

4.4 Numerical simulations

At this point it may be useful to briefly consider an example of numerical simulation based on the mathematical model of the evolution of the process. The result of this simulation is shown in Fig. 2, where the physical parameters (shown in Table 4) are taken from the second experiment of oil A (see [2]).

Table 4 Physical parameters of the numerical simulation. D_G is the segregated wax diffusivity.

$T_e = 293$ K	$T_i = 278$ K	$R_i = 0.05$ m
$R_e = 0.12$ m	$C_s(T_i) = 20.1 \ \frac{\text{kg}}{\text{m}^3}$	$c^*_{\text{tot}} = 20.25 \ \frac{\text{kg}}{\text{m}^3}$
$b_w = 0.006 \ \frac{\text{kg}}{\text{m}^3 \cdot \text{K}}$	$D_w = 3.20 \times 10^{-7} \ \frac{\text{m}^2}{\text{s}}$	$D_G = 1.4 \times 10^{-8} \ \frac{\text{m}^2}{\text{s}}$

In Fig. 2 the mass deposited per unit surface (rescaled by $C_s(T_i)R_i \approx 1$ kg/m^2) is shown as a function of time (rescaled by $R_i^2/D_w \approx 2.2$ h). Crosses represent the experimental data, while the solid line is the result of simulation. Experimental data correspond to 4, 6, and 19 hours. In Fig. 2 we can identify Stages 1 and 2 (characterized by linear growth) and Stage 3, where the growth rate tends asymptotically to 0. In this example the system evolves from Stage 1, since the difference $c^*_{\text{tot}} - C_s(T)$ is positive both at the cold and at the warm wall.

Another (and simpler) method to predict the amount of deposit for a specific oil can be the one based on the extrapolation procedure described in Appendix 2. This method essentially permits to predict the asymptotic behaviour from the linear growth phase by approximating the curve describing the deposit with an exponential branch. This procedure has shown to fit well the experimental data also for oil A where asymptotic mass measures are available.

The plot (based on the extrapolation procedure of Appendix 2) describing the mass deposit growth for oil A is shown in Fig. 3.

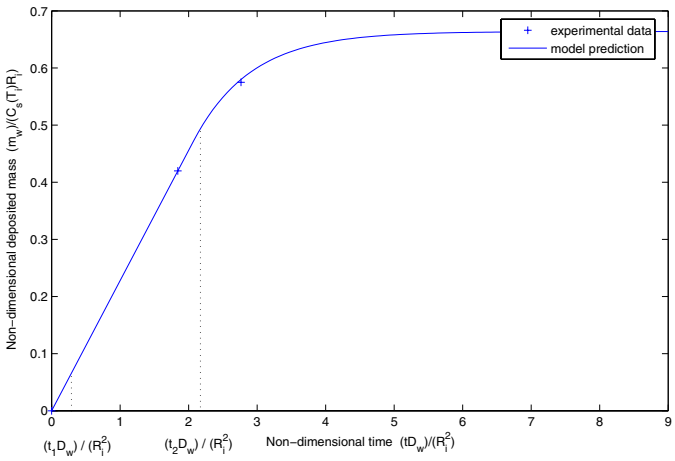

Fig. 2 Numerical simulation. Experimental data refers to Oil A.

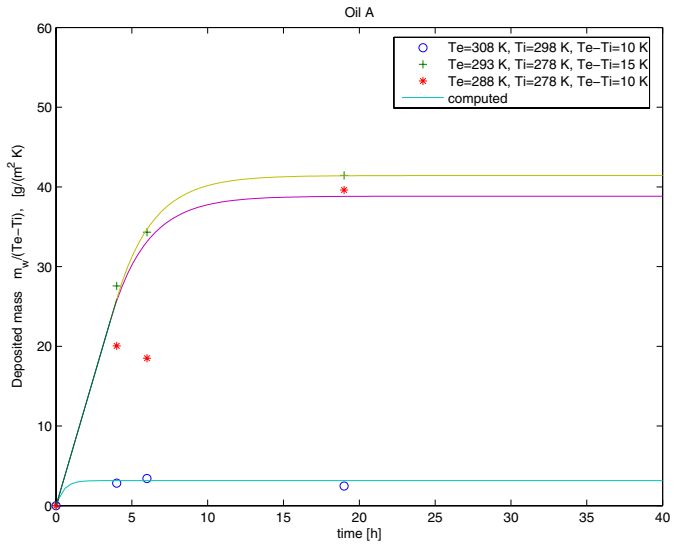

Fig. 3 Extrapolation of asymptotic mass from the stage of linear regime (Appendix 2).

5 Conclusions and perspectives

We have studied the static cold finger apparatus with the aim of using the experimental data (deposited wax as a function of time) in order to derive the coefficient D_w of molecular diffusion of the dissolved wax. We have shown that a simple model incorporating the basic phenomena can be set up such that

- It explains that m_w grows linearly in a time interval $(0, t_2)$, then it tends asymptotically to a value $m_{w\infty}$.
- From the values $m_{w\infty}$ corresponding to two different cold wall temperatures the solubility curve of wax in oil can be linearly interpolated (see eq. (12)).
- From the knowledge of $m_w(t)$ in the time interval of linear growth $(0, t_2)$ and from the above mentioned interpolation, the value of D_w can be calculated (see eq. (15)).
- The values obtained for D_w are systematically larger than expected. This seems to indicate that in the static device only the most mobile fraction of wax migrates during the measurements time. Moreover the presence of possible convective motions increases the temperature gradient at the cold wall implying that D_w is overestimated. The discussion performed in Appendix 3 confirms this interpretation on the basis of a completely different argument.

We have seen that it always exists a stage in which a desaturation front moves inwards and separates an inner zone where segregated wax exists from an outer zone where the wax only exists in a dissolved phase. We have described a method for deducing the asymptotic deposited mass from the analysis of the stage of linear growth of the deposit.

A suggestion for further experiments is to analyze by physical/chemical methods the composition of the deposit. In this way a model including classes of wax components could be formulated. An alternative procedure would be to operate with an artificial mono-component migrating species in a mono-component solvent.

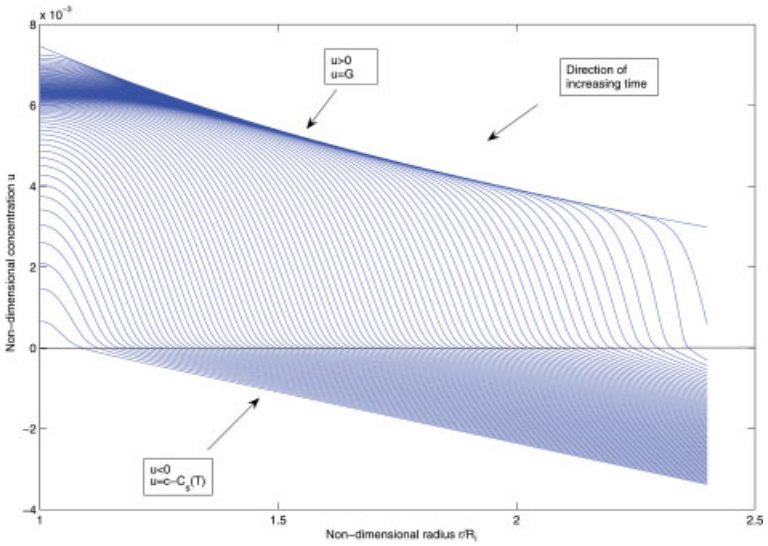

Fig. 4 Plot of function u defined in (35) during Stages 1 and 2.

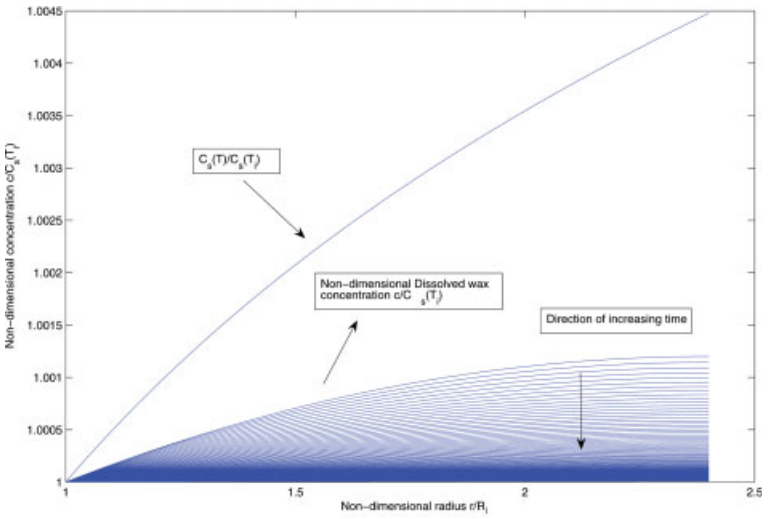

Fig. 5 Plot of function $c/C_s(T_i)$ during Stage 3.

Appendix 1

The profiles of G, c have been computed using the nondimensional variables $G/C_s(T_i)$, $c/C_s(T_i)$, T/T_i, and the rescaled coordinates r/R_i, $t/(R_i^2/D_w)$. It is convenient to introduce the function

$$u(r,t) = \begin{cases} G(r,t), & 1 < r < s(t), \quad t_1 < t < t_2, \\ \\ c(r,t) - C_s(T(r)), & s(t) < r < R_e/R_i, \quad t_1 < t < t_2, \end{cases} \tag{35}$$

to study Stages 1 and 2, noting that the sign of u is associated to the saturation state ($u = G > 0$ during Stage 1, while in Stage 2 $u > 0$ in the saturated region, $u < 0$ in the unsaturated region).

In Fig. 4 the profile of function $u(r,t)$, defined in (35), is plotted. Of course the branches $u > 0$ correspond to $G(r,t)$, while $u < 0$ correspond to $c - C_s(T)$. The physical parameters are the ones shown in Table 4. Stage 3 is described in Fig. 5, where the profile of $c(r,t)$ is plotted, showing its asymptotic limit.

Appendix 2

Here we give a procedure to determine the parameter b_w in the absence of experimental data for asymptotic masses. This procedure is the one we have used to derive the values of parameter b_w in Table 1 for oils B, C, D, F, E of [2]. The procedure is tested for oil A (Fig. 3) with excellent agreement. To determine the parameter b_w we use a method that extrapolates the evolution of $m_w(t)$ during Stage 3 on the basis of the data acquired during the phase of linear growth (Stages 1 and 2).

Among the solutions of the diffusion equation

$$\frac{\partial c}{\partial t} - D_w \mathrm{div}(\nabla c) = 0$$

satisfying conditions

$$c(R_i, t) = C_s(T_i), \qquad \left.\frac{\partial c}{\partial r}\right|_{r=R_e} = 0,$$

we seek those that can be written as the product of a function of time t and a function of r. Referring to nondimensional variables $\hat{t} = t(D_w/R_i^2)$, $\hat{r} = r/R_i$, $\hat{c} = (c - C_s(T_i))/C_s(T_i)$ the equation becomes

$$\frac{\partial \hat{c}}{\partial \hat{t}} - \frac{1}{\hat{r}} \frac{\partial}{\partial \hat{r}} \left(\hat{r} \frac{\partial \hat{c}}{\partial \hat{r}} \right) = 0$$

and we look for solutions of type $\hat{c} = \Theta(\hat{t}) F(\hat{r})$ such that

$$\hat{c}(1) = 0, \qquad \left.\frac{\partial \hat{c}}{\partial \hat{r}}\right|_{\hat{r}=R_e/R_i} = 0.$$

We get

$$\hat{c}(\hat{r}, \hat{t}) = \hat{U}(\hat{r}) \exp\{-\alpha^2 (\hat{t} - \hat{t_2})\},$$

with $\hat{U}(\hat{r})$ solution of the Bessel equation

$$\frac{d^2 \hat{U}}{d\hat{r}^2} + \frac{1}{\hat{r}} \frac{d\hat{U}}{d\hat{r}} + \alpha^2 \hat{U} = 0, \qquad \hat{U}(1) = 0, \qquad \frac{d\hat{U}}{d\hat{r}} \left(\frac{R_e}{R_i} \right) = 0.$$

Therefore

$$\hat{U}(\hat{r}) = Y_o(\alpha) J_o(\hat{r}\alpha) - J_o(\alpha) Y_o(\hat{r}\alpha),$$

where J_o and Y_o are the zero order Bessel functions of first and second kind. The parameter α is obtained solving the eigenvalues problem

$$Y_o(\alpha) J_o' \left(\frac{R_e}{R_i} \alpha \right) - J_o(\alpha) Y_o' \left(\frac{R_e}{R_i} \alpha \right) = 0.$$

Clearly, being interested in the asymptotic phase, we will consider only the dominant eigenvalue α_o, which is the smallest. With $R_e/R_i = 2.4$ we get $\alpha_o = 0.94$. Going back to the original variables, the attenuation factor is

$$\exp\left\{ -\alpha_o^2 \frac{D_w}{R_i^2} (t - t_2) \right\}.$$

Now we look for a match between the linear part of $m_w(t)$ and the asymptotic value in the form

$$m_w(t) = m_w(t_2) + \tau\gamma \left[1 - \exp\left(-\frac{t - t_2}{\tau} \right) \right], \tag{36}$$

where $m_w(t)$ is the deposited wax per unit surface, t_2 is the final time of Stage 2 (i.e. the desaturation time) and

$$\tau = \frac{R_i^2}{D_w \alpha_o^2}, \qquad \gamma = \dot{m}_w(t_2).$$

The asymptotic deposited wax per unit surface then is given by

$$m_{\infty w} = m_w(t_2) + \dot{m}_w(t_2) \frac{R_i^2}{D_w \alpha_o^2}$$

and recalling that (see 14))

$$\dot{m}_w(t_2) = D_w b_w \frac{(T_e - T_i)}{\ln\left(\dfrac{R_e}{R_i}\right)} \frac{1}{R_i}$$

we get

$$m_{\infty w} = m_w(t_2) + b_w \frac{(T_e - T_i)}{\ln\left(\dfrac{R_e}{R_i}\right)} \frac{R_i}{\alpha_o^2}.$$

The unknown D_w does not appear in the expression for $m_{\infty w}$. Using two different temperatures at the cold finger $T_{i1} > T_{i2}$ we get

$$b_w = \left[\frac{R_e^2 - R_i^2}{2R_i} - \frac{R_i}{\ln\left(\dfrac{R_e}{R_i}\right)\alpha_o^2} \right]^{-1} \cdot \frac{m_{wT_{i2}} - m_{wT_{i1}}}{T_{i1} - T_{i2}} =: \chi \cdot \frac{m_{wT_{i2}} - m_{wT_{i1}}}{T_{i1} - T_{i2}} \tag{37}$$

where χ is just a geometric factor - in our case $\chi = 18.40$ m^{-1} - and $m_{wT_{i1}}$ and $m_{wT_{i2}}$ represent the deposited wax per unit surface at the desaturation time for the experiments with temperatures T_{i1} and T_{i2}. Finally we can deduce D_w from the measures of $\dot{m}_w$ and plot the asymptotic part of $m_w(t)$ on the basis of the data of the linear part.

It is very important to observe that this procedure reproduces the evolution of $m_w(t)$ in a satisfactory way in particular for the only case (oil A) in which asymptotic measures of the deposit are really available.

Appendix 3

Here we present a procedure for determining an upper bound for wax diffusivity D_w. Performing the overall mass balance of G during Stage 1 (i.e. integrating (21) over $R_i < r < R_e$, $0 < t < t_1$, and using the initial and boundary conditions (22)-(24)) we obtain

$$\int_{R_i}^{R_e} rG(r,t_1)dr = \int_{R_i}^{R_e} rG_o(r)dr - \frac{D_w b_w (T_e - T_i)}{\ln\left(\dfrac{R_e}{R_i}\right)} t_1. \tag{38}$$

Passing to Stage 2, we integrate (25) over $R_i < r < s(t)$, $t_1 < t < t_2$, using (27)-(29). We get

$$\int_{R_i}^{R_e} rG(r,t_1)dr = -\int_{t_1}^{t_2} D_G s \frac{\partial G}{\partial r}(s,t)dt. \tag{39}$$

From (29), recalling that $\dfrac{\partial c}{\partial r}(s,t) > 0$, we deduce that

$$-D_G s \frac{\partial G}{\partial r}(s,t) < D_w b_w s \frac{dT}{dr}(s) = \frac{D_w b_w (T_e - T_i)}{\ln\left(\dfrac{R_e}{R_i}\right)}. \tag{40}$$

Combining (38), (39), (40) we have the inequality

$$D_w > \frac{1}{t_2} \frac{\ln\left(\dfrac{R_e}{R_i}\right)}{b_w(T_e - T_i)} \int_{R_i}^{R_e} rG_o(r)dr, \tag{41}$$

where, from (22),

$$\int_{R_i}^{R_e} rG_o(r)dr = \frac{R_e^2 - R_i^2}{2}\left[c^*_{\rm tot} - C_s(T_i) + \frac{1}{2}\frac{b_w(T_e - T_i)}{\ln\left(\dfrac{R_e}{R_i}\right)}\right] - \frac{R_e^2}{2}b_w(T_e - T_i). \tag{42}$$

Using the parameters of oil A (see Table 4) with $t_2 = 5$ h we obtain the estimate

$$D_w > 2.90 \times 10^{-7} \ \frac{\rm m^2}{\rm s}. \tag{43}$$

It has to be remarked that this estimate is based just on one experimental information, that is desaturation time, a quantity that can be read on Fig. 3 with reasonable accuracy.

To obtain an upper bound for D_w we observe that the deposited mass (per unit surface) at time t_2 must be smaller than the total amount of wax in the system at time $t = 0$. Thus

$$\frac{2D_w b_w(T_e - T_i)t_2}{\ln\left(\dfrac{R_e}{R_i}\right)} < c^*_{\rm tot}(R_e^2 - R_i^2), \tag{44}$$

leading to inequality

$$D_w < \frac{c^*_{\rm tot}(R_e^2 - R_i^2)\ln\left(\dfrac{R_e}{R_i}\right)}{2b_w t_2(T_e - T_i)}. \tag{45}$$

With the same values introduced above we obtain

$$D_w < 6.5 \times 10^{-5} \ \frac{\rm m^2}{\rm s}. \tag{46}$$

The a priori estimate obtained for D_w (in particular the lower estimate (43), which is very close to the value shown in Table 2) seems to confirm that in the static device deposition is produced by the migration of a lighter, more mobile fraction of wax.

References

[1] E. D. Burger, T. K. Perkins, and J. H. Striegler, Studies of wax deposition in the trans Alaska pipeline, Journal of Petroleum Technology, 1075–1086 (1981).

[2] S. Correra, M. Andrei, and C. Carniani, Wax diffusivity: is it a physical property or a pivotable parameter? Petroleum Science and Technology **21** (9), 1539–1554 (2003).

[3] S. Correra, A. Fasano, L. Fusi, and D. Merino-Garcia, Calculating deposit formation in the pipelining of waxy crude oils, Meccanica (to appear).

[4] A. Fasano, L. Fusi, and S. Correra, Mathematical models for waxy crude oils, Meccanica **39**, 441–483 (2004).

[5] A. Fasano and M. Primicerio, Heat and mass transfer in non-isothermal partially saturated solutions, Recent Trends in Mathematical Physics (to appear).

[6] A. Fasano and M. Primicerio, Temperature driven mass transport in concentrated saturated solutions, Progress in Nonlinear Differential Equations and their Applications **61**, 91–108 (2005).

[7] M. V. Kok and O. Saracoglu, Mathematical modelling of wax deposition in crude oil pipeline system, SPE **64514**, 1–7 (2000).

[8] D. A. Shock, J. D. Sudbury, and J. J. Crockett, Studies on the mechanism of paraffin deposition and its control, Journal of Petroleum Technology **7** (9), 23–30 (1955).

[9] J. S. Weintgarten and J. A. Euncher, Methods for predicting wax precipitation and deposition, SPE Prod. Eng., 121–126 (1988).

[10] C. H. Wu, J. L. Creek, K. S. Wang, R. M. Carlson, S. Cheung, P. J. Shuler, and Y. Tang, Measurements of wax deposition in paraffin solutions, AIChE Proceedings of the 4th International Symposium on Wax Thermodynamics and Deposition (2002).

